NeuroImage 327 (2026) 121714

Contents lists available at ScienceDirect

NeuroImage

journal homepage: www.elsevier.com/locate/ynimg

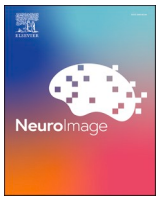

An intracranial insight into (the timing of) the action observation network

Maria Del Vecchio [a,*], Fausto Caruana [a], Flavia Maria Zauli [b], Veronica Pelliccia [c], Ivana Sartori [c], Piergiorgio d'Orio [a,c], Francesca Talami [a], Simone Del Sorbo [a,d], Davide Albertini [e], Giacomo Rizzolatti [a,e], Pietro Avanzini [a]

[a] Istituto di Neuroscienze, Consiglio Nazionale delle Ricerche 43125, Parma, Italy
[b] Università degli Studi di Milano, Dipartimento di Scienze Biomediche e Cliniche "L. Sacco" 20157, Milano, Italy
[c] Centro per la Chirurgia dell'Epilessia "Claudio Munari", Ospedale Ca' Granda—Niguarda 20162, Milano, Italy
[d] School of Advanced Studies, Università di Camerino, 62032, Camerino (MC), Italy
[e] Università di Parma, Dipartimento di Medicina e Chirurgia, 43125 Parma, Italy

ARTICLE INFO

Keywords:
Mirror mechanism
Temporal bonding
Congruence
Action execution
Sensorimotor cortex

ABSTRACT

The Action Observation Network (AON) is a large-scale brain network that supports the perceptual encoding and recognition of actions performed by others. The identification of the nodes of the human AON has been clarified over the past 30 years thanks to the high spatial resolution of neuroimaging techniques. The temporal dynamics underpinning their activations is in contrast still unsettled, because of methodological constraints. Here we investigate the timing of the AON components by intracranially recording gamma-band oscillations from 23 drug-resistant epileptic patients during the observation, and execution, of naturalistic, complex actions (including reaching, grasping, and object manipulation). Our analysis enabled us to decompose the AON into 10 distinct spatio-temporal clusters, five of which are composed of multiple cortical territories that are synergistically activated. The resulting four-dimensional representation of the AON, examined alongside its counterpart during the execution of the same action, highlights the specific functions fulfilled by each territory, distinguishing regions that process lower-order visual aspects from those that mirror specific aspects of the action. These include two spatio-temporal clusters located in dorsal and ventral fronto-parieto-temporal territories, specifically encoding the reaching phase (dorsal) and the object-contact phase (ventral). A third cluster, confined to the posterior perisylvian region, is associated with object manipulation. Overall, our work brings out the overlooked temporal details of the AON in humans and assesses their relationship with the execution of a real-time full-fledged action, spotlighting the importance of a fourth dimension in investigating the motor system.

1. Introduction

Between 1992 and 1996, the Neuroscience team of the University of Parma identified in the monkey premotor area F5 the *mirror neurons*, a class of motor neurons responding not only to action execution but also to the observation of others actions in the absence of any overt movement of the monkey (Di Pellegrino et al. 1992; Gallese et al. 1996; Rizzolatti et al. 1996). Since that discovery, a massive body of literature has documented that multiple fronto-parietal regions of the human brain are endowed with mirror properties (Rizzolatti et al., 2014), composing, together with temporal regions, the rich cortical network responsive to action observation (Action Observation Network, AON), whose topography has been repeatedly investigated by neuroimaging meta-analyses (Caspers et al. 2010; Hardwick et al. 2018; Molenberghs et al. 2012).

Our knowledge of the temporal activation profiles of the different

Abbreviations: AE, Action Execution; AIP, Anterior IntraParietal; AO, Action Observation; AON, Action Observation Network; CBCT, Cone-Beam Computed Tomography; ECoG, Electrocorticography; EEG, Electroencephalography; FEF, Frontal Eye Field; FFC, Fusiform Face Complex; GBP, Gamma-Band Power; IEDs, Ictal Epileptic Discharges; LED, Light Emitting Diode; MEG, Magnetoencephalography; LIPv, Area Lateral Intraparietal Ventral; MEP, Motor Evoked Potential; MIP, Medial IntraParietal; MST, Medial Superior Temporal Area; MT, Middle Temporal; PEF, Premotor Eye Field; PIT, Poterior Infero-Temporal; TMS, Transcranial Magnetic Stimulation; TPOJ1, Area TemporoParietal Occipital Junction 1; TPOJ2, Area TemporoParietal Occipital Junction 2; SCEF, Supplementary and Cingulate Eye Field; sEEG, Stereo-Electroencephalography; SPL, Sound Pressure Level; VIP, Ventral IntraParietal Complex.

* Corresponding author at: Via Volturno 39/E, 43125 Parma, Italy.
E-mail address: maria.delvecchio@in.cnr.it (M. Del Vecchio).

https://doi.org/10.1016/j.neuroimage.2026.121714
Received 19 March 2025; Received in revised form 14 November 2025; Accepted 12 January 2026
Available online 13 January 2026

nodes of the AON is considerably limited relative to its topographic distribution. Neuroimaging techniques lack, indeed, the temporal resolution needed to resolve the fast neural dynamics characterizing the processing of observed actions (Qin et al. 2023; Perry et al. 2018; Caruana et al. 2017). In principle, electroencephalography (EEG) or magneto-electroencephalography (MEG) meet these temporal requirements, yet they are unable to render a spatially-resolved picture of cortical areas. These *limitations* could be overcome by testing the cortical responsiveness to action observation via invasive recordings like intracranial EEG, which combines a millisecond temporal resolution with the precise localization of the explored cortical sites. Caruana and coworkers (2017) administered several videos of manual actions to 49 patients undergoing stereo-electroencephalography (sEEG) and demonstrated that different events (onset of the video, start of the hand movement, contact between the hand and the object) trigger the neural activity of different cortical networks, thus suggesting that the response to action observation is not unitary but rather characterized by multiple components attuned to specific features of the action. A similar conclusion was reached by Perry and collaborators (2018, see also Dreyer et al. 2023), who measured electrocorticography (ECoG) in 7 subjects, proving that sensorimotor, parietal, and frontal neural populations respond with different timings relative to the onset of the hand action video. Finally, Qin and colleagues (2023) adopted ECoG in 10 subjects to demonstrate that the temporal interplay between motor and visual cortices is action-dependent, especially when comparing unexpected vs. predictable observed actions.

An open question in understanding the timing of brain responses to action observation is whether distinct temporal profiles are shared across different cortical regions, independently of their anatomical proximity. In other words, we lack a time-resolved picture of the functional responses during action observation, where each pool of regions is also accompanied by a specific time course informative of the underlying functional properties (Del Vecchio and Avanzini, 2020).

Another unsettled issue concerns the degree of the temporal matching between the neural activation profiles elicited during action observation with those recruited during action execution. This aspect has been preliminarily addressed by an intracranial EEG study (Del Vecchio et al. 2020), demonstrating a reliable correspondence in the activation time courses proper of action observation and execution for the secondary somatosensory cortex, a region known to exhibit mirror properties. A few studies on macaques found that the ventral premotor cortex (F5), but not other premotor areas, exhibits neural population dynamics partly shared between execution and observation, suggesting that a possible common coding might be area-specific (Albertini et al. 2021; Ferroni et al. 2021; Jerjian et al. 2020; Jiang et al., 2020; Mazurek et al. 2018; but see Pomper et al., 2023). Bringing this type of investigation to human intracranial recordings has the potential to assess the topography of the observation/execution temporal matching, further revealing whether specific areas or time courses are common between the two conditions.

Starting from these premises, the present study aims to a) render a resolved picture of the AON temporal dynamics during the observation of hand actions including reaching, grasping and object manipulation and b) test throughout the AON whether the time course underlying action observation matches that proper of action execution. To this aim, we enrolled a cohort of 23 right-handed drug-resistant epileptic patients undergoing left-hemisphere sEEG investigation, and asked them to observe and execute manipulative actions. First, we explored and clustered the temporal behavior of each AON subdivision. Second, we documented the degree of temporal similarity between observation/execution across the cortical fields responsive to action observation. Finally, we investigated the responsiveness of each region to different types of sensory stimulations (i.e. visual, acoustic, and somatosensory) to provide not only a brain-wise map of the degree of matching in the neural response to action observation and execution but also cues about the functional properties possibly explaining high similarity scores.

2. Methods

2.1. Participants

Stereo-electroencephalography data were collected from left-implanted 23 right-handed patients (13 females, *see* Table T1 in Supplementary Materials for further details) suffering from drug-resistant focal epilepsy (age 35± 8). Patients were stereotactically implanted with intracerebral electrodes as part of their presurgical evaluation at the Centro per la Chirurgia dell'Epilessia "Claudio Munari" (Ospedale Ca' Granda-Niguarda, Milan, Italy). Implantation sites were selected solely on clinical grounds, using seizure semiology, scalp-EEG, and neuroimaging as guides. Patients were fully informed regarding the electrode implantation and sEEG recording, and informed consent was obtained. The present study received the approval of the Ethics Committee of the Ospedale Ca' Granda - Niguarda (ID 939–2.12.2013). Intracerebral recordings were performed according to the sEEG methodology to define the cerebral structures involved in the onset and propagation of seizure activity. Neurological examination was unremarkable for all patients and, in particular, no patient presented any motor or sensory deficits.

2.2. Electrode implantation and anatomical reconstruction

Patients were implanted with depth electrodes each having a diameter of 0.8 mm and consisting of contacts 2 mm long and spaced 1.5 mm apart (DIXI Medical, Besancon, France). Immediately after the implantation, cone-beam computed tomography (CBCT) was obtained with an O-arm scanner (Medtronic) and registered to pre-implantation three-dimensional (3D) T1-weighted MR images. Subsequently, multimodal scenes were built with the 3D Slicer software package, and the exact position of each contact was determined, at the single patient level, looking at multiplanar reconstructions. In addition, the transformation needed to switch from the individual anatomy to the fs-LR-average brain template was also applied to the cortical localization of each recording contact, so as to have the chance to merge contacts from all patients onto a common template, thus obtaining a population picture to be compared with previous findings about the action observation network. The anatomical reconstruction procedure adopted in this study is the same as presented in (Avanzini et al. 2016).

2.3. Experimental design

Patients were required to observe a reach-to-grasp-and-manipulative action performed by the experimenter (*Observation Condition*), while sitting next to them so to experience the other's movement from a first-person perspective, which is known to enhance motor reactivity to action observation (Angelini et al., 2018; Ge et al. 2018; Maeda et al. 2002). The session was composed of 60 trials, 20 for each of the three objects positioned on a workbench (a screw, a nail, or a bolt), presented in random order. Each trial comprised three different phases whose onset and offset were signaled by digitally captured events: i) a preparation phase, ii) a reach-to-grasp phase and iii) a manipulation phase. The experimenter had first to press a button box with the right hand, which in turn triggered the turning on of one of the LEDs placed in correspondence with the three objects, thus signaling which object the experimenter had to manipulate (i.e., tighten a screw, beat a nail or screw a bolt with the hand). The experimenter had to press the button and thus hold the action until the LED turned off, i.e. for a fixed duration of 2 s, ensuring a motor preparation phase in which they could plan the upcoming action without any overt movement of the right arm. When the light turned off, the experimenter was free to start the reach-to-grasp movement at an individual pace. When the experimenter's hand reached the object, a photocell placed on the workbench signaled the end of the reaching and the beginning of the manipulative phase. After two seconds from this event, an auditory cue signaled to the experimenter the end of

the action and they had to return to the starting position for the next trial. The same experimental procedure was then executed by the patient with his/her right hand (*Execution Condition*). Fig. 1 illustrates the procedure.

2.4. Clinical and neurophysiological tests

The day after the implantation, patients admitted to the neurology ward underwent clinical and neuropsychological tests to functionally characterize the recording contacts. In particular, patients were administered with the following stimuli.

Acoustic stimulation: Patients wearing earphones were required to listen to 100-click acoustical stimulation delivered in the right ear at 85 dB SPL (*Sound Pressure Level*).

Median nerve stimulation: The right median nerve was stimulated at the wrist, using 100 constant-current pulses (0.2-ms duration) at 1 Hz while the patient lied in bed with eyes closed. The intensity and exact site of stimulation were varied until an observable thumb twitch was obtained. The stimulation intensity was set at 10 % above the motor threshold to avoid habituation effects.

Visual flash: Patients wearing goggles received 100 bilateral visual stimulations at a rate of 1 Hz (intensity set at 3cd/m^2).

All the simulations were delivered by means of a Nihon-Khoden Neuropack M1 machine, allowing the user to search for threshold values and control stimulation intensity and/or frequency.

2.5. SEEG data

For each patient, the initial recording procedure included the selection of an intracranial reference, which was chosen by using both anatomical and functional criteria. The reference was computed as the average of two adjacent contacts both exploring white matter. These contacts were selected time-by-time among those neither exhibiting response to standard clinical simulations, including somatosensory (median, tibial, and trigeminal nerves), visual (flash), and acoustical (click) stimulations nor evoking any sensory and/or motor behaviors upon electrical stimulation. The sEEG trace was recorded with a Neurofax EEG-1100 (Nihon Kohden System) at a 1-kHz sampling rate. Clinicians visually inspected recordings to verify for ictal epileptic discharges (IEDs) during the stimulation protocol. No patients presented IEDs during the recording of the experiment.

2.6. Data processing

Data on the AON were extracted according to the following procedure. First, we superimposed the AON, as defined by Hardwick and coworkers (2018), with the parcellation developed by Glasser and co-authors (Glasser et al., 2016). This first step allowed us to identify 84 anatomo-functional fields belonging to the AON territories. Among these, we selected the anatomo-functional fields with at least 20 % of the nodes explored by the AON, resulting in an overall number of 41 areas investigated. The sEEG data were then analyzed in all patients whose implantation, co-registered on a template, included contacts exploring the AON-related anatomo-functional fields.

The signal from each contact was transformed into time-frequency plots using complex Morlet wavelet decomposition with 4 cycles. Gamma-Band Power (GBP) was extracted across 10 adjacent, non-overlapping 10 Hz frequency bands from 55 to 145 Hz for each phase (preparation, reaching-to-grasp, and manipulation) in observation and execution conditions (un-normalized). GBP was also analogously computed for the baseline condition, ranging from 350 ms to 50 ms before the LED lighting. To normalize the amplitude of the data across patients and contacts, power in each frequency in post-stimulus bins was transformed into z-scores relative to the baseline interval ([−350, −50] ms before the light indicating the object that is to be manipulated turns on) and then averaged across frequencies. The same pipeline was applied for the analysis of both action observation and execution.

As for the peripheral stimulations (median nerve, acoustical, and visual stimulations), the selected window for GBP computation ranged from 100 ms before to 500 ms after the stimulus delivery (see Avanzini et al. 2016; 2018; Del Vecchio et al. 2019). Since the reaching-to-grasp phase has a variable duration (patients were instructed to initiate the movement after the LED turned off, starting and moving at their own pace), we identified separately for the observation and the execution condition the outliers as the trials whose duration exceeded the first or the third quartiles of half their difference (i.e., an outlier was a trial whose duration exceeded $q3 + w \times (q3 - q1)$ or was less than $q1 - w \times (q3 - q1)$, where w was set at 1.5 and q1 and q3 were respectively the first and the third quartiles) and excluded the whole trial for further analysis. We standardized the trial duration for the remaining trials by linearly interpolating the GBP time course at $n = 152$ points (representing the top of the distribution, max duration = 1518 ms, minimum duration = 875 ms, average duration 1159 ± 132 ms). In this way, we could compare the time course across trials and contacts, regardless of

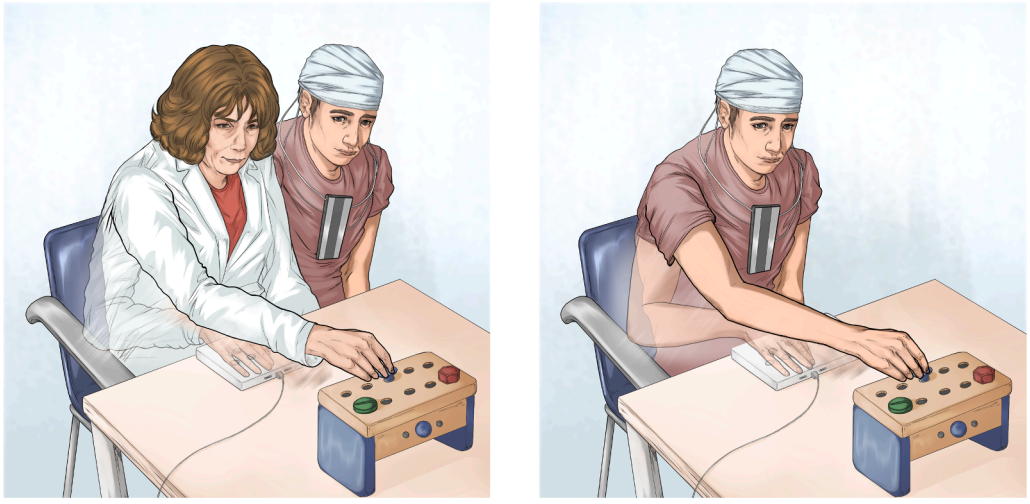

Fig. 1. The experimental procedure. During the preparation phase, the participant is instructed to press and hold a button box with their right hand while fixating on an LED that signals the object to be manipulated (lasting 2 s). Once the LED switches off, the participant can release the button at their own pace and initiate a reach toward the object (reaching-to-grasp phase). This phase concludes when the participant's hand passes through a photocell positioned just above the objects, marking the onset of hand-object interaction. In the final manipulation phase, the participant must manipulate the object continuously for 2 s, completing the trial.

the variability naturally affecting real motor execution. Finally, to compare contacts between observation and execution conditions, we applied the same procedure to the reaching-to-grasp phase of the execution, whose duration values were highly comparable (max duration = 1588 ms, minimum duration 677 ms, average duration 1080 ± 164 ms).

2.7. Statistics and reproducibility

Subsequently, to identify the responsive contacts, the gamma band power in each post-stimulus bin was compared against a zero-mean distribution using a one-tailed *t*-test ($p < 0.001$). In each phase, contacts were identified as significant if they presented at least three significant time bins.

To investigate the temporal coherence across areas within AON, we first computed the average time course of all the contacts significantly responding to at least one phase of the observation condition. To increase the consistency of the results, we submitted to this stage only areas including at least two contacts responding significantly to action observation. Subsequently, Pearson correlation was applied on the averaged time-course (across leads) for each region to evaluate the degree of similarity of the whole temporal dynamics of the action across different areas, obtaining a squared, symmetrical correlation matrix. To increase the reliability of the correlation results, we displayed only values reaching the statistical significance ($p < 0.05$) and whose R absolute value exceeded 0.3. To sort the areas according to their intrinsic correlation, data were hierarchically clustered (distance: euclidean, nearest neighbor linkage). This allowed functionally related clusters of areas to emerge as high-scores squares arranged along the diagonal of the correlation matrix, highlighted in the dendrogram using a cutoff of 1 (average linkage method, cutoff selected as the closest to average fusion distance). In addition, to verify the robustness of the temporal similarity analysis beyond Pearson correlation, we also applied Dynamic Time Warping (DTW) on the same averaged time courses (see Fig. 1 of Supplementary Materials). GBP time courses were further averaged according to the identified clusters to characterize the prototypical temporal profiles and their significance was tested (one tailed *t*-test, $p < 0.01$). Significance lasting <50 ms were not shown.

Regarding responsiveness to basic stimulations, AON contacts were labeled as responsive only if three consecutive time-bins were significant, in analogy with previous works of our group (Avanzini et al. 2016; 2018). Both data processing and statistical analyses were performed with Matlab R2022b. The visualization of contacts on the cortical sheet were obtained with Caret software (Van Essen 2012).

3. Results

3.1. Database

The data were analyzed from 23 patients whose implanted electrodes overlap with the 41 anatomo-functional fields occupied by the AON of upper limb actions (Hardwick et al. 2018, *see* Fig. 2A-B). Overall, 376 contacts exploring the gray matter were identified within the AON areas (in blue).

3.2. Sampling and reactivity of AO network

Thirty-four out of 41 regions were included in our analysis. These comprised territories within the fronto-parietal network and temporal regions, considered key hubs of the AON. In contrast, seven regions (i.e., VIP, V4t, 7AL, PIT, LO1, 7PL, V8) were not sampled. Additionally, four regions (i.e., FST, 6v, IFJa, IFSp) were excluded as they did not contain significant contacts in any phase, while five others (i.e., 7 PC, 55b, IFJp, MT, SCEF) were excluded due to the limited number ($n < 2$) of significant contacts. In total, 25 regions were included in the subsequent analyses. Table T2 in the Supplementary Materials reports the number of

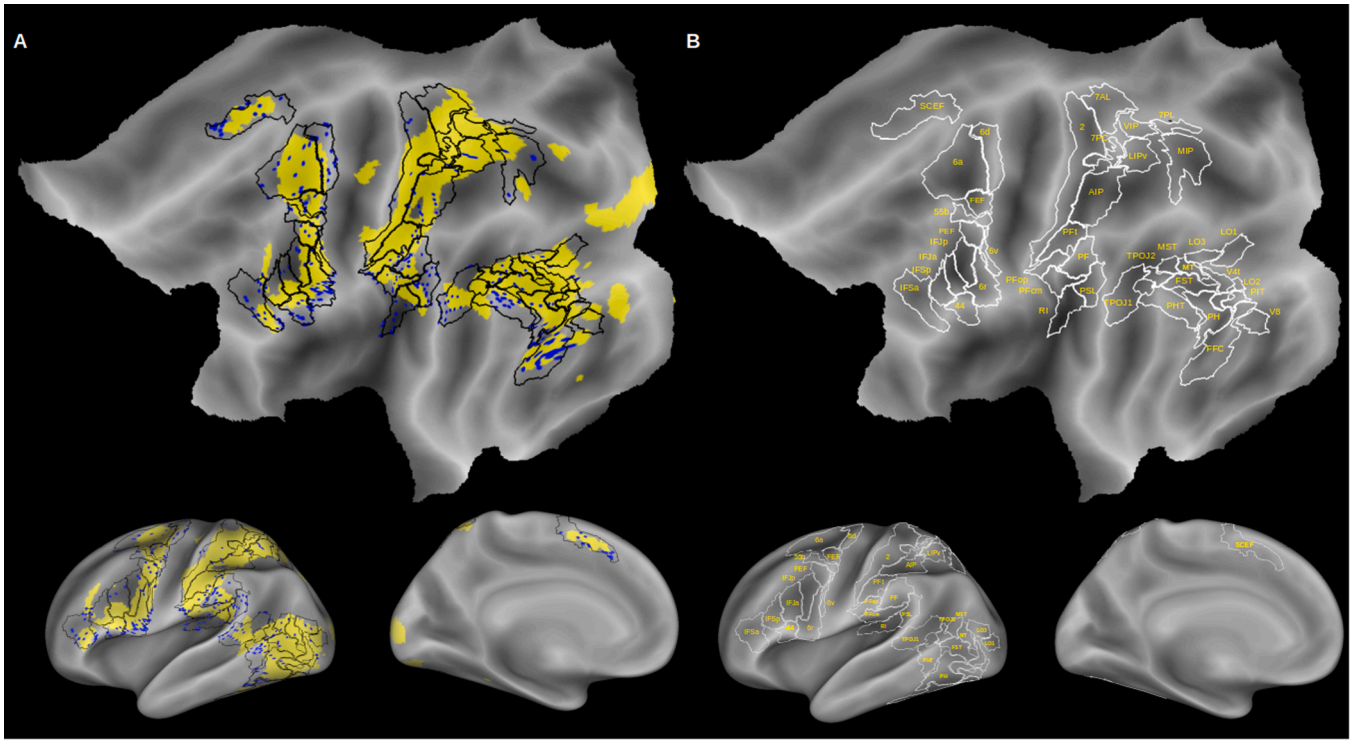

Fig. 2. Action observation network and sampling. Panel A shows the AON identified by Hardwick and co-authors (in yellow) on a flat map, along with the sampled contacts located within these regions (blue dots). Black borders delineate the 41 regions in which the AON has been subdivided, including only those with at least 20 % of their nodes sampled. Panel B displays the names of these 41 anatomo-functional fields, based on the parcellation by Glasser et al. (2016). For both panels, lateral and mesial views are shown on inflated cortical surfaces at the bottom.

responsive contacts out of the total sampled contacts for each region, presented both as absolute values and as a percentage of the total sampled. During the central phase of the observed action, i.e., the reaching-to-grasp phase, we observed the largest number of responsive leads within the AON, making this phase the most strongly represented across our recordings. In this interval, responsive leads were distributed across nearly all fronto-parietal and temporal nodes, with only a few exceptions (PEF, IFSa, and MIP). By contrast, the preceding (preparation) and following (manipulation) phases were associated with a smaller number of responsive leads within the AON and, notably, with no significant recruitment in the dorsal premotor cortex. More specifically, the preparation phase showed a predominance of responsive

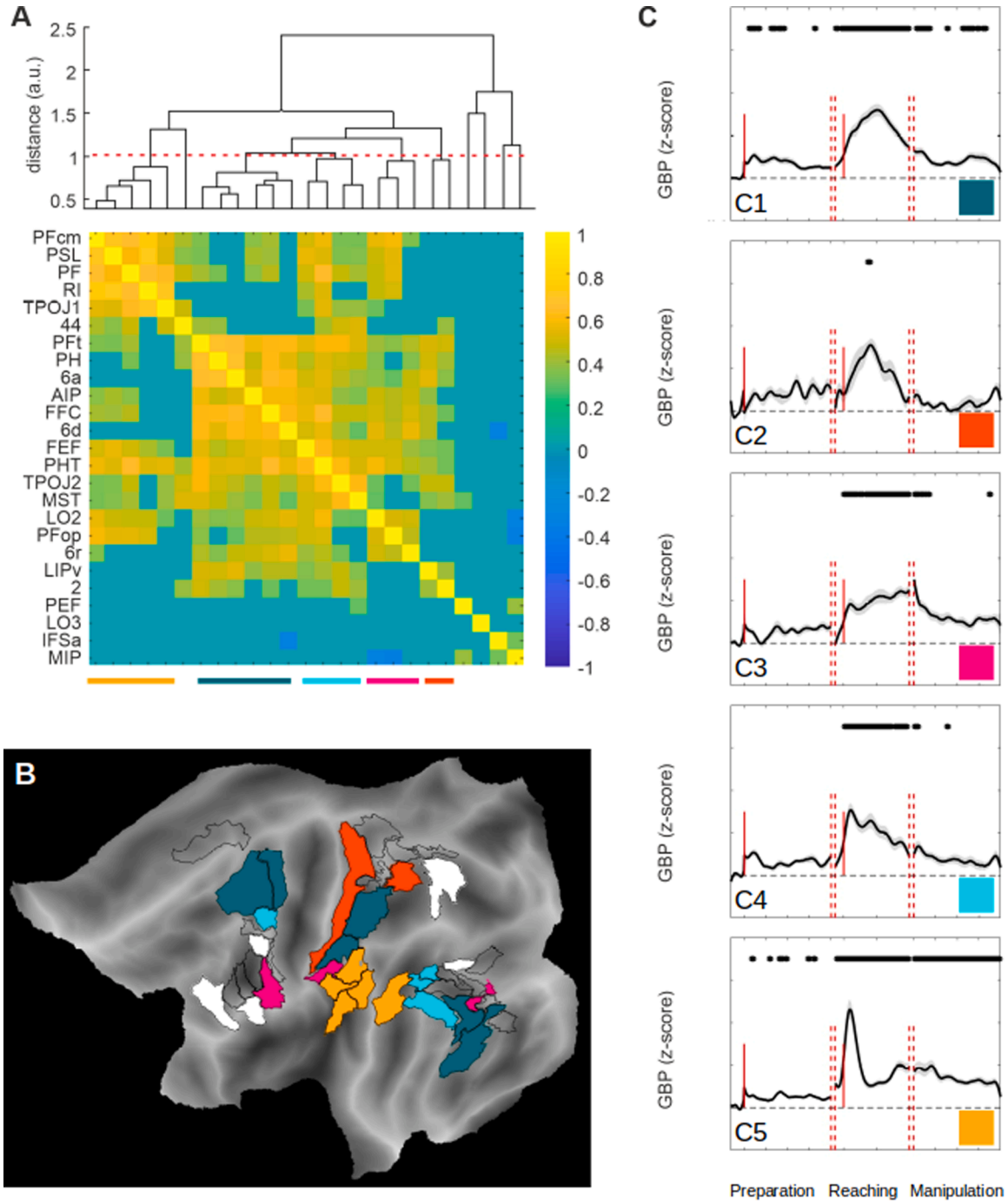

Fig. 3. AON temporal coherence during action observation Panel A shows the correlation values (R) among the considered parcels for the observed full-fledged action. The corresponding hierarchical cluster (cutoff = 1) is displayed above the correlation matrix. Correlations that were not significant ($p > 0.05$) or that fell within the range [−0.3, 0.3] were set to zero for visualization purposes. Panel B displays, on a flat map, the five clusters identified in the correlation matrix using the same color code, while responsive parcels not grouped into clusters are shown in white. For each of the five cortical clusters, the averaged GBP time courses are shown for all action phases (preparation, reaching-to-grasp, manipulation), using the same color code as in Panel C. The squares displayed for each cluster in Panel C follow the same color scheme presented below the correlation matrix. Significant bins relative to baseline lasting <50 ms are not displayed. For each phase (including baseline), a moving average filter was applied to the time courses of individual contacts within the area ($n = 25$ points for the three phases; $n = 10$ points for baseline) before averaging them at the cluster level to generate the figure. Solid red vertical lines indicate, from left to right, the onset of the preparation and reaching-to-grasp phases. Dashed vertical lines separate the three experimental phases.

leads in temporal regions, with only sparse involvement of frontal (IFSa) and intraparietal (MIP) sites. The manipulation phase, instead, was marked by a progressive reduction of responsive leads in temporal nodes and by a stronger contribution of parietal regions (see Fig. 2 of Supplementary Materials).

3.3. Response profiles during action observation

The analysis of the temporal progression of the activated nodes, obtained using a dendrogram clustering a correlation matrix (cutoff of 1.0), identified 10 distinct activation profiles. Five of these (C1-C5, Fig. 3) were shared by multiple fields distributed over different frontal, parietal, and temporal sectors, and deserve a specific description here below. The remaining five temporal profiles (C6-C10), in contrast, were relative to five individual regions, namely, the BA44, PEF, LO3, IFSa and MIP. Their temporal courses, depicted in Fig. 3 of Supplementary Materials, are suggestive of a contribution in visual and oculomotor behavior, and are further described in the relative caption.

Among the five multiregional clusters, C1 were constituted by some of the key-hubs of the AON, including the dorsal premotor regions 6d and 6a, and inferior parietal/intraparietal regions (AIP and PFt) and, at the temporal level, FFC and PH. All these areas were characterized by a sustained increase in gamma-band power (GBP) throughout the reaching-to-grasp phase, especially in its central part. The GBP modulation was minimal during the preparatory phase, whereas activity re-emerged at the end of the manipulation phase, as evidenced by a return to significance in the late manipulation phase. A similar GBP profile across the different action phases was also evident in C2, encompassing the primary somatosensory area BA2 and LIPv. Given these features, we will refer to C1 and C2 as the *dorsal AON*.

Cluster C3 included the ventral premotor region 6r and the inferior parietal PFop. Moreover, a comparable GBP profile was observed in one inferior temporal region (LO2). In these regions, GBP remained significantly above baseline throughout the reaching-to-grasp and manipulation phases, with a peak at the time of hand-object interaction. The tuning of this temporal profile on the hand-object interaction induced us to label C3 as ventral AON.

Cluster C4 was mainly composed of posterior middle temporal regions (PHT, TPOJ2, and MST). Its GBP profile showed a sudden, steep response onset at the beginning of the reaching-to-grasp phase, with activity returning to baseline only during the manipulation phase. A smaller component, yet not significant, was also visible at the beginning of the preparatory phase, betraying a possible visual origin due to the temporal coincidence with the instruction LED turning on. In light of this evidence, it is not surprising that the same cluster also includes only one specific frontal region, i.e. the frontal eye fields (FEF), which contributes in controlling gaze and eye movements. These considerations led us to label C4 as the optokinetic AON.

As shown in Fig. 3, although clusters C1–C4 are functionally distinct at the 1.0 threshold, they all originate from a common branch of the dendrogram, likely reflecting their minimal GBP modulation during action preparation and their marked increase during the reaching-to-grasp phase. In contrast, cluster C5 was positioned separately from the others and comprised posterior perisylvian regions. Its temporal profile showed a significant increase in GBP that persisted throughout the reaching-to-grasp and manipulation phases. In line with previous reports (Del Vecchio et al., 2020), two components are observed: a steep, large-amplitude transient at the beginning of the reaching-to-grasp phase, and a second, lower-amplitude component that spans the approach of the object and the entire manipulation phase. Based on this morphology, we labeled C5 as the haptic AON.

The somatosensory, visual and auditory origin of the activities reported above has been further corroborated by clinical and neurophysiological tests conducted in accordance with previous SEEG studies (Del Vecchio et al. 2020), whose results are available in Supplementary Materials (Supplementary Figure 4 and Supplementary Table 4).

3.4. Correlation between action observation and execution

To investigate the functional overlap between the time course characterizing action observation and execution, we analyzed the correlation coefficient between AO and AE conditions. Fig. 4 shows, for each region, the correlation coefficient in a color scale ranging from yellow to black. These correlations encompassed the entire action, including all three phases of the experimental procedure.

Despite the consistent temporal course during action observation, the *dorsal AON* exhibited different matching degrees between observation and execution. Indeed, C1 showed a high correlation (range 0.4–0.6) in its frontal, parietal and temporal sectors. As in the case of AO, AE peaked in the reaching-to-grasp phase of the action, albeit the activation started with a peak at the onset of this epoch, followed by a sustained activity lasting until the end of the manipulatory phase. The contrast between the reaching-to-grasp and the manipulatory phases was indeed less sharp in the AE condition, suggesting more uniform activation in action execution along the whole action dynamics. It is worth noting that although two-thirds of this cluster consisted of regions associated with sensorimotor control (e.g., premotor cortices), the amplitude recorded during observation and execution was comparable. Conversely, C2, centered on somatosensory and superior parietal regions, displayed in contrast a low correlation (below 0.2) between AO and AE. Indeed, the time course underlying action execution had a biphasic profile, with a first tonic peak during the action onset and a second one initiating around the manipulatory phase and sustained until the end of the action. More importantly, the amplitude recorded during the execution phase showed higher GBP z-score values compared to those observed during the observation phase. Collectively, these results are coherent with a predominant role of C2 in the somatosensory feedback, peaking at the action onset (tactile-off from the keyboard when lifting the hand) and constantly activated by the haptic feedback during the manipulation.

The *ventral AON* (C3) also showed a high correlation (range 0.4–0.6) between AO and AE, despite minor but interesting divergences between execution and observation. In particular, data showed that, during action execution, the resulting time course is similar to the one of C2, with a biphasic activation in analogy with the other clusters.

The *optokinetic AON* (C4), anchored to the posterior middle temporal regions and FEF, showed a mixed activation profiles, with superior temporal regions (i.e. PHT) exhibiting a very high correlation (above 0.6) between AO and AE, and MST and LO3 showing a lower correlation (below 0.2). At a more general level, in both observation and execution, C4 was typified by a weak but very distinct peak at the beginning of the preparatory phase, and by a quick onset of a second boost of activity at the onset of the reaching-to-grasp phase, lasting until the end of the action. Note that during AE, C4 activation is kept high throughout the execution time, unlike during AO, where instead there is a gradual decrease in activation.

Finally, the *haptic AON* (C5) also showed a very high correlation, with regions above 0.6 between AO and AE, both showing a phasic peak at the onset of the action. As for the case of C4, the time course during action execution was partially similar to the one recorded from somatosensory regions in C2, namely, a biphasic profile peaking at the onset of the reaching-to-grasp and manipulatory phase, and sustained until action offset. In contrast to C4 and C2, however, the amplitude of the signal was the highest during action observation. The correlation Pearson's R coefficient for the comparison between observation and execution (full-fledged action) for each area is detailed in Table T3 of Supplementary Materials.

4. Discussion

The cortical network underlying other's action observation in humans has been delineated by several imaging studies (Caspers et al., 2010; Hardwick et al. 2018; Molenberghs et al. 2012), and the

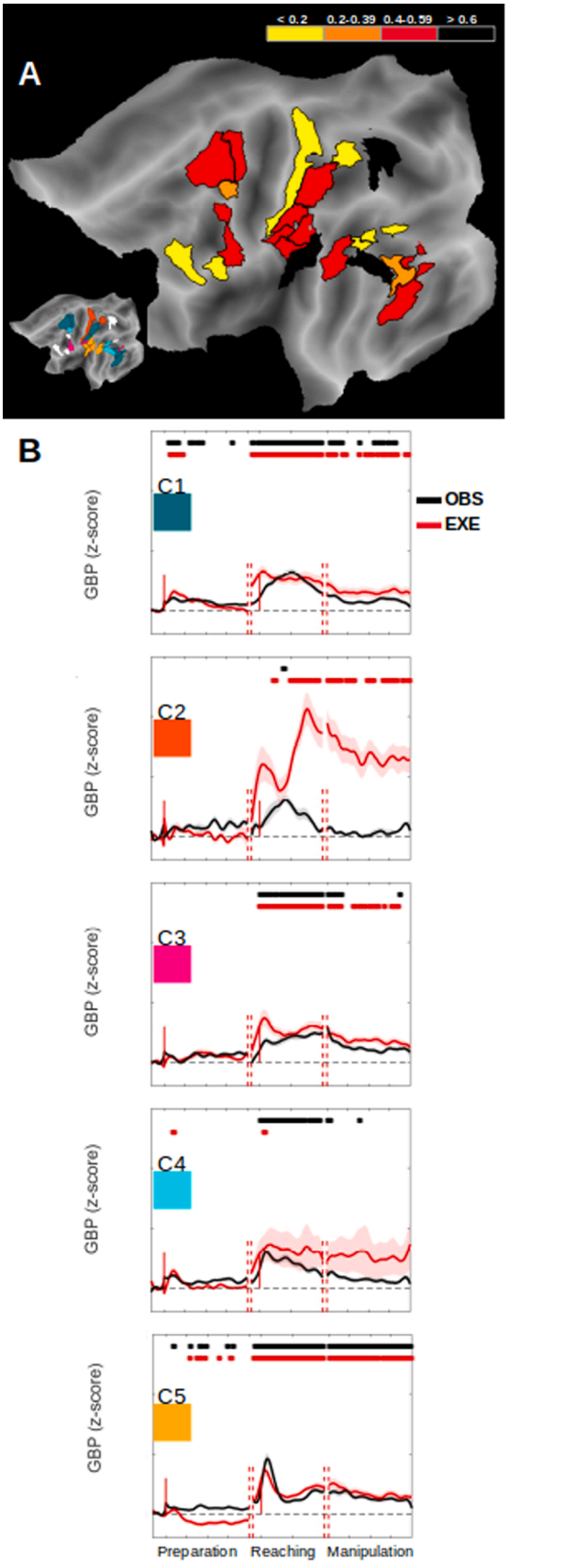

(caption on next column)

Fig. 4. Temporal bonding between action observation and execution. Panel A reports the R values within each area (i.e. values on the diagonal of Panel A) from higher values of R (in black) to lower values (in yellow). In detail: black $R \geq 0.60$, red $R = [0.4, 0.59]$, orange $R = [0.2, 0.39]$ and yellow $R < 0.2$. For completeness, the left inset of Panel A reports on a flat map the previously identified five identified clusters (see Fig. 3, panel B). Panel B reports for the previously underlined clusters the GPB temporal course for the full-fledged action (black trace: observation, red trace: execution). Significance with respect to the baseline lasting >50 ms is shown in the correspondent color code. For each phase (including baseline), a moving average filter was applied to the time courses of individual contacts within the area ($n = 25$ points for the three phases; $n = 10$ points for baseline) before averaging them at the cluster level to generate the figure. Solid red vertical lines indicate, from left to right, the onset of the preparation and reaching-to-grasp phases. Dashed vertical lines separate the three experimental phases.

functional properties shared by both action observation and execution have been reported by both scalp EEG (e.g. mu rhythm, Angelini et al. 2018; Avanzini et al. 2012; Debnath et al. 2019; Fox et al. 2016; Muthukumaraswamy et al. 2004) and intracerebral studies (Dreyer et al. 2023; Mukamel et al., 2010; Perry et al. 2018). Indirect evidence of a motor mirror mechanism in humans also comes from TMS studies, which report increased MEPs (Motor Evoked Potentials) during action observation (Fadiga et al., 1995; Naish et al. 2014; Patuzzo et al. 2003). However, these studies do not describe the dynamic behavior of the AON during the observation of a full-fledged action performed by a conspecific, preventing them from inferring its specific role based on its temporal course. In addition, most studies have used video-recorded stimuli rather than live actions, which maximizes reproducibility across trials but reduces ecological validity, as real-life actions naturally vary across occurrences. Here, the cluster analysis of the activation profiles allowed us to dissect the AON response into multiple multi-areal clusters encoding specific aspects of the observed action. While only left-hemisphere implanted patients were included—given that the execution condition involved the right hand—the AON is known to be bilaterally represented (Caspers et al., 2010; Hardwick et al. 2018; Molenberghs et al. 2012), suggesting that the reported dynamics might be potentially generalized between hemispheres.

The *dorsal AON* consists of dorsal premotor, inferior parietal, and inferotemporal regions. The comparison of its time-course during AO and AE shows that the contribution of this network in these two conditions is not completely overlapping. In fact, the first peak at the onset of the executed action, which is absent in the observation, shows the presence of a somatosensory component - a finding also confirmed by the result of peripheral stimulations (see Supplementary Materials). Within the *dorsal AON*, C2 represents the somatosensory component of the AO primarily including somatosensory and superior parietal regions. The contribution of somatosensory regions to action observation has already been emphasized by previous neuroimaging studies (Gazzola and Keysers, 2009; Keysers et al. 2004; Turella et al., 2012; see also Keysers et al. 2010). Our results thus confirm these observations, but also show that these areas remain modulated primarily during execution, with the time course during action observation characterized by a limited number of sites showing significant responses and a weakly significant temporal progression as well, leaving primary somatosensory regions only marginally involved in processing actions performed by others.

The *ventral AON*, encompassing the ventral premotor cortex and inferior parietal lobule, corresponds to another key subnetwork of the mirror neuron system. Of this network our data suggest that, as with *dorsal AON*, there is a similar but not identical contribution during AO and AE, with an early peak in AE reflecting a somatosensory component. During AE, activity remains constant during both reach-to-grasp and manipulation, more so than in the other clusters. This is in line with what we know about the ventral premotor cortex mirror neurons that respond to both grasping and specific manipulation (Mazurek et al.

2018). Furthermore, in a previous sEEG study we have shown that inferior parietal cortex, especially PFop, not only responds during action observation but does it so even more strongly if the action is performed using tools, leading us to conclude that this node plays an important role in remembering motor programs involved in complex actions (Caruana et al. 2017).

Here, we cannot retract from highlighting the parallelism with the hypotheses that Rizzolatti and Matelli advanced in 2003 about the organization of the dorsal visual stream. Indeed, they proposed that the dorsal visual stream and its recipient parietal areas form two distinct functional systems: the dorso-dorsal stream - mainly responsible for the online control of action - and the ventro-dorsal stream, mostly involved in encoding grasping and object prehension (Rizzolatti and Matelli 2003). Such a bifurcation reflects faithfully into the topography and time courses of the dorsal and ventral AON clusters. Indeed, the former has a reactivity peaking in the middle of the reaching phase, while the latter is attuned to the hand-object contact. Overall, we demonstrated that the features indicated by single neuron studies on non human primates pertain also to the organization of the human motor system, being visible through intracerebral recordings.

The *optokinetic AON*, centered primarily on the posterior middle temporal gyrus, appears to reflect mainly the visual processing of the moving stimuli, in strict coordination with the oculomotor behavior. Its temporal node, in fact, corresponds to the regions typically referred to as the visual hub of the AON (Caspers et al. 2010). Its frontal node, on the other hand, involves the FEF region, largely known to mediate oculomotor behavior (Borra and Luppino, 2021) and thus not surprisingly coordinating its time course with the temporal regions encoding visual motion. This cluster is a clearcut example of how grouping cortical regions based on their time course allows to reveal functional synergies beyond the sole connectivity (Del Vecchio and Avanzini, 2020). Finally, *the haptic AON* is a perisylvian cluster characterized by a sustained activity starting in correspondence of the hand-object interaction and lasting until the end of the manipulation, extending previous results underlined for the sole SII (Del Vecchio et al. 2020). The notion of a circuit specifically responding during the observation of others' sensations and actions involving haptic control has been reported in both human and non-human primates (*see* Keysers et al. 2010), corroborating the idea that the role of this network extends well-beyond pure somatosensation.

In addition to these main clusters, our analysis isolated five additional clusters (C6-C10) composed of single regions: MIP and PEF, active strongly during the preparation phase; area 44, exhibiting a marked activation only during the observation condition; and the last two - ISFa and LO3, presenting a marginal activation during the reaching phase.

Taken together, here we provide a four-dimensional, time-resolved representation of the AON, complementing the static picture offered by neuroimaging studies. Our data challenge the idea that the AON is a monolithic unit, but rather it represents the synergistic behavior of different streams, often anatomically distant, which operate in parallel with temporally—and therefore functionally—analogous activities. In addition, when comparing the time courses of action observation with those exhibited during execution, each module shows peculiar and non-overlapping activity that we address in the next section.

4.1. A brain-distributed motor resonance

The concept of a "*mirror system*," commonly used to describe the fronto-parietal component of the AON, seems to suggest a perfect overlap between the neural activity evoked during the execution of a certain action and its observation. While the overlap principle applies very well to the spatial domain, with the topographic congruence between responses to AO and AE witnessed by several neuroimaging studies and meta-analyses (Caspers et al., 2010; Hardwick et al. 2018; Molenberghs et al. 2012), whether a similar overlap is also found in the temporal organization of the neural response remains an underexplored issue (Del Vecchio et al., 2020; Dreyer et al. 2023; Mukamel et al., 2010; Perry et al. 2017; Pomper et al. 2023). Indeed, the evaluation of a possible temporal match between executed and observed actions has been often overlooked because of the insufficient temporal resolution of the approaches commonly employed in human neuroscience, not to mention the technical challenges posed by the capability to record brain activity during the execution of complex ecological behaviors (*but see* Brandi et al. 2014). SEEG, thanks to its high spatiotemporal resolution, is in the ideal position to tackle this fundamental issue. Given the chance to record the activity of the AON via SEEG, we took the opportunity to evaluate the degree of temporal matching between AO and AE at the micro-regional level, with temporal discrepancies between AO and AE that are still informative about the different functions performed by each system in different contexts.

Our data demonstrate that the temporal profiles of the gamma-band activity recorded during AO and AE from each cluster exhibit both similarities and specificities, making a case for common and different contributions of the same network to action execution and observation. On one hand, most regions of the AON show a significant correlation in time between AO and AE, indicating that the motor response during action observation instantiates a temporal dynamics that resembles - at a macroscopic level - that proper of action execution. Notably, the use of live observation instead of video recordings embedded our observation trials with a natural variability, making even more salient the temporal similarity across conditions, as it cannot be ascribed solely to the mere concatenation of evoked activities. On the other hand, a significant correlation between AE and AO indicates that the overarching dynamics during the unfolding of an action—whether executed or observed—are shared, but this does not imply that the responses are identical or lack features specific to each condition. From this consideration, in the following sections we will examine each cluster individually.

The *dorsal AON* (C1) displays a significant correlation between AO and AE throughout the entire action unfolding, with a prominent difference concerning the reaching onset. While in AO, the dorsal AON shows a peak of activity in the middle of the reach-to-grasp phase, in AE, its activity peaks already at the action onset. We speculate that the contribution of the dorsal AON to AO is temporally delayed with respect to AE because, in the former case, the recruitment of the motor program corresponding to the observed action can only come after such observed action has been initiated, whereas during execution this information is obviously available only since the onset of the action. One could argue that the activity of the dorsal AON hosts a major somatosensory/proprioceptive component given that the activity around the action onset timing is almost exclusive for action execution. However, this hypothesis can be ruled out by contrasting the activity of C1 with C2, which, because of its topography, can be considered the somatosensory branch of the AON (Gazzola and Keysers 2009; Keysers et al. 2010). Indeed, C2 activity is characterized by two peaks, the first at the beginning of the action onset (as in C1) and the second, larger peak (absent in C1) close to the hand-object interaction. The temporal similarity between C1 and C2 is negligible, and nonetheless, the temporal congruency between AO and AE is sustained in C1 and null for C2. Overall, we can thus regard the dorsal AON as a hub instantiating a common motor representation during AO and AE, with somatosensory information adding on in action execution mainly confined to predominantly somatosensory areas.

Concerning the *ventral AON*, there is a similar but not identical co-activation profile during AO and AE, with an early peak at the action onset only characterizing AE and likely reflecting a somatosensory component and a second peak common to both conditions that is precisely centered on the grasping time. Unlike C1, however, in C3 the activity remains constant during both reach-to-grasp and hand-object interaction, coherently with single-neuron studies in non-human primates showing that these areas house neurons firing during both hand grasping and manipulation (Maranesi et al. 2015; Mazurek et al. 2018).

The last two clusters, namely the *optokinetic AON* and *haptic AON*, are less represented in the action observation literature. The former shows a

significant correlation predominantly due to a sustained activity lasting for the whole action. However, despite a larger variability, a stronger activation is visible during AE than AO, in particular during the manipulation phase. While this finding may seem counterintuitive at first glance, it is not if one considers the constant visual feedback functional to action monitoring provided by these regions during action execution (Ogawa et al. 2006). Of note, this profile not only characterizes the posterior middle temporal region but also the anterior branch of the same cluster, that corresponds to the FEF. Concerning the haptic AON, this perisylvian cluster displays the highest level of correlation between AE and AO, peaking at the action onset. Perisylvian regions are widely recruited following tactile stimulation, and more relevantly, they play a role in managing high-order somatosensory information and gating them toward a distributed brain circuitry (De Haan and Dijkerman, 2020; Del Vecchio et al., 2021).

4.2. The value of SEEG in providing a fine-grained, ecological perspective on motor functions

Contemporary cognitive neuroscience strongly advocates for ecological and naturalistic approaches (Shamay-Tsoory and Mandelsohn, 2019; Gothard et al., 2018), which require experimental paradigms mimicking or even incorporating real-life actions and allowing participants to act in an out-of-the-lab multisensory environment. This demand is especially urgent in the neuroscience of action execution and action observation whose studies, except for those on nonhuman primates, have been characterized by a paradoxical absence of movement. An even greater challenge is to do all this while not losing spatial and, more importantly, temporal resolution. Indeed, the ideal aim of an ecological approach to action neuroscience is to fully characterize the cortical control of action both in terms of topography and temporal dynamics (Del Vecchio and Avanzini, 2020; Mercier et al. 2022; Rizzolatti et al. 2018).

Our experimental approach moves in this direction, offering an ecological insight into investigating the brain circuitry subtending action observation and execution. Here, we analyzed the neural activity of the brain regions known to be recruited during the observation of others' actions to investigate (a) the anatomo-functional degree of homogeneity of this network, particularly with regard to temporal profiles of activation, and (b) the similarities and misalignments in the temporal dynamics between action execution and observation. On the one hand, our approach allowed us to show that the AON is not a unitary entity, but that conversely it is possible to dissect this network into multiple spatiotemporal units, distributed over different fronto-parieto-temporal territories. On the other hand, it provides the chance to assess the similarity and difference between action observation and execution, making a case for the pivotal role of the temporal dimension in revealing the functional role of the sensorimotor regions pertaining to the AON.

5. Limitations

Some cortical regions are sampled with a relatively small number of electrode contacts. This stems from our decision to adopt a parcellation strategy with fine-grained regions of interest, which allows a more precise functional characterization but inevitably reduces the number of observations per parcel. While this approach maximizes spatial specificity, it may limit the generalizability of our findings, as conclusions regarding certain regions are based on fewer implanted contacts.

Data statement

The selection of patients has been submitted to a series of stringent precautionary measures. The conditions of our ethics approval do not permit public archiving of individual anonymized raw data. Readers seeking access to the data should contact the corresponding author. Access will be granted to named individuals in accordance with ethical procedures governing the reuse of sensitive data. Specifically, requestors must sign a formal agreement confirming that (a) the user may not use the database for any non-academic purpose (b) the document must be signed by a person with a permanent position at an academic institute or publicly funded research institute. Up to five other researchers affiliated with the same institute for whom the signee is responsible may be named at the end of this document which will allow them to work with this dataset. The user may not distribute the database or portions thereof in any way.

CRediT authorship contribution statement

Maria Del Vecchio: Writing – review & editing, Writing – original draft, Visualization, Formal analysis, Data curation. **Fausto Caruana:** Writing – review & editing, Writing – original draft. **Flavia Maria Zauli:** Writing – review & editing, Writing – original draft, Investigation, Data curation. **Veronica Pelliccia:** Writing – review & editing, Writing – original draft, Investigation, Data curation. **Ivana Sartori:** Writing – review & editing, Writing – original draft, Investigation, Data curation. **Piergiorgio d'Orio:** Writing – review & editing, Writing – original draft, Investigation, Data curation. **Francesca Talami:** Writing – review & editing, Writing – original draft, Data curation, Conceptualization. **Simone Del Sorbo:** Writing – review & editing, Writing – original draft, Data curation. **Davide Albertini:** Writing – review & editing, Writing – original draft, Visualization, Data curation. **Giacomo Rizzolatti:** Writing – review & editing, Writing – original draft, Data curation, Conceptualization. **Pietro Avanzini:** Writing – review & editing, Writing – original draft, Supervision, Project administration, Funding acquisition, Data curation.

Declaration of competing interest

The authors declare no competing interest.

Acknowledgements

MDV was supported by the European Union Horizon 2020 Framework Program through grant agreement no 935539 (Human Brain Project, SGA3). MDV (since June 2023) and SDS were supported by the Project EBRAINS-Italy (IR00011) from the Italian Ministry of University and Research. DA was supported by #NEXTGENERATIONEU (NGEU) and funded by theMinistry of University and Research (MUR), National Recovery and Resilience Plan (NRRP), project MNESYS (PE0000006 – A Multiscale integrated approach to the study of the nervous system in health and disease (DN. 1553 11.10.2022). F.M.Z. was supported by ERC-2022-SYG Grant number 101071900 Neurological Mechanisms of Injury and Sleep-Like Cellular Dynamics (NEMESIS).PA was supported by HORIZON-INFRA-2022 SERV (GrantNo.101147319) "EBRAINS 2.0: A Research Infrastructure to Advance Neuroscience and Brain Health.

Supplementary materials

Supplementary material associated with this article can be found, in the online version, at doi:10.1016/j.neuroimage.2026.121714.

References

Albertini, D., Lanzilotto, M., Maranesi, M., Bonini, L., 2021. Largely shared neural codes for biological and nonbiological observed movements but not for executed actions in monkey premotor areas. J. Neurophysiol. 126, 906–912. https://doi.org/10.1152/jn.00296.2021.

Angelini, M., Fabbri-Destro, M., Lopomo, N.F., Gobbo, M., Rizzolatti, G., Avanzini, P., 2018. Perspective-dependent reactivity of sensorimotor mu rhythm in alpha and beta ranges during action observation: an EEG study. Sci. Rep. 8, 12429. https://doi.org/10.1038/s41598-018-30912-w.

Avanzini, P., Fabbri-Destro, M., Dalla Volta, R., Daprati, E., Rizzolatti, G., Cantalupo, G., 2012. The dynamics of sensorimotor cortical oscillations during the observation of

hand movements: an EEG study. PLoS. One 7, e37534. https://doi.org/10.1371/journal.pone.0037534.
Avanzini, P., Abdollahi, R.O., Sartori, I., Caruana, F., Pelliccia, V., Casaceli, G., Mai, R., Lo Russo, G., Rizzolatti, G., Orban, G.A., 2016. Four-dimensional maps of the human somatosensory system. Proc. Natl. Acad. Sci. 113. https://doi.org/10.1073/pnas.1601889113.
Avanzini, P., Pelliccia, V., Lo Russo, G., Orban, G.A., Rizzolatti, G., 2018. Multiple time courses of somatosensory responses in human cortex. Neuroimage 169, 212–226. https://doi.org/10.1016/j.neuroimage.2017.12.037.
Borra, E., Luppino, G., 2021. Comparative anatomy of the macaque and the human frontal oculomotor domain. Neurosci. Biobehav. Rev. 126, 43–56. https://doi.org/10.1016/j.neubiorev.2021.03.013.
Brandi, M.-L., Wohlschläger, A., Sorg, C., Hermsdörfer, J., 2014. The neural correlates of planning and executing actual tool use. J. Neurosci. 34, 13183–13194. https://doi.org/10.1523/JNEUROSCI.0597-14.2014.
Caruana, F., Avanzini, P., Mai, R., Pelliccia, V., LoRusso, G., Rizzolatti, G., Orban, G.A., 2017. Decomposing tool-action observation: a stereo-EEG study. Cereb. Cortex. 27, 4229–4243. https://doi.org/10.1093/cercor/bhx124.
Caspers, S., Zilles, K., Laird, A.R., Eickhoff, S.B., 2010. ALE meta-analysis of action observation and imitation in the human brain. Neuroimage 50, 1148–1167. https://doi.org/10.1016/j.neuroimage.2009.12.112.
Debnath, R., Salo, V.C., Buzzell, G.A., Yoo, K.H., Fox, N.A., 2019. Mu rhythm desynchronization is specific to action execution and observation: evidence from time-frequency and connectivity analysis. Neuroimage 184, 496–507. https://doi.org/10.1016/j.neuroimage.2018.09.053.
de Haan, E.H.F., Dijkerman, H.C., 2020. Somatosensation in the brain: a theoretical re-evaluation and a new model. Trends Cogn. Sci. 24, 529–541. https://doi.org/10.1016/j.tics.2020.04.003.
Del Vecchio, M., Avanzini, P., 2020. La Recherche du Temps Perdu: timing in Somatosensation. Commentary: somatosensation in the brain: a theoretical re-evaluation and a new model. Front. Syst. Neurosci. 14. https://doi.org/10.3389/fnsys.2020.597755.
Del Vecchio, M., Caruana, F., Sartori, I., Pelliccia, V., Lo Russo, G., Rizzolatti, G., Avanzini, P., 2019. Ipsilateral somatosensory responses in humans: the tonic activity of SII and posterior insular cortex. Brain Struct. Funct. 224, 9–18. https://doi.org/10.1007/s00429-018-1754-6.
Del Vecchio, M., Caruana, F., Sartori, I., Pelliccia, V., Zauli, F.M., Lo Russo, G., Rizzolatti, G., Avanzini, P., 2020. Action execution and action observation elicit mirror responses with the same temporal profile in human SII. Commun. Biol. 3, 80. https://doi.org/10.1038/s42003-020-0793-8.
Del Vecchio, M., Fossataro, C., Zauli, F.M., Sartori, I., Pigorini, A., d'Orio, P., Abarrategui, B., Russo, S., Mikulan, E.P., Caruana, F., Rizzolatti, G., Garbarini, F., Avanzini, P., 2021. Tonic somatosensory responses and deficits of tactile awareness converge in the parietal operculum. Brain 144, 3779–3787. https://doi.org/10.1093/brain/awab384.
di Pellegrino, G., Fadiga, L., Fogassi, L., Gallese, V., Rizzolatti, G., 1992. Understanding motor events: a neurophysiological study. Exp. Brain Res. 91, 176–180. https://doi.org/10.1007/BF00230027.
Dreyer, A.M., Michalke, L., Perry, A., Chang, E.F., Lin, J.J., Knight, R.T., Rieger, J.W., 2023. Grasp-specific high-frequency broadband mirror neuron activity during reach-and-grasp movements in humans. Cereb. Cortex. 33, 6291–6298. https://doi.org/10.1093/cercor/bhac504.
Fadiga, L., Fogassi, L., Pavesi, G., Rizzolatti, G., 1995. Motor facilitation during action observation: a magnetic stimulation study. J. Neurophysio. 73 (6), 2608–2611. https://doi.org/10.1152/jn.1995.73.6.2608.
Ferroni, C.G., Albertini, D., Lanzilotto, M., Livi, A., Maranesi, M., Bonini, L., 2021. Local and system mechanisms for action execution and observation in parietal and premotor cortices. Curr. Biol. 31, 2819–2830. https://doi.org/10.1016/j.cub.2021.04.034 e4.
Fox, N.A., Bakermans-Kranenburg, M.J., Yoo, K.H., Bowman, L.C., Cannon, E.N., Vanderwert, R.E., Ferrari, P.F., van IJzendoorn, M.H., 2016. Assessing human mirror activity with EEG mu rhythm: a meta-analysis. Psychol. Bull. 142, 291–313. https://doi.org/10.1037/bul0000031.
Gallese, V., Fadiga, L., Fogassi, L., Rizzolatti, G., 1996. Action recognition in the premotor cortex. Brain 119, 593–609. https://doi.org/10.1093/brain/119.2.593.
Gazzola, V., Keysers, C., 2009. The observation and execution of actions share motor and somatosensory voxels in all tested subjects: single-subject analyses of unsmoothed fMRI data. Cereb. Cortex. 19, 1239–1255. https://doi.org/10.1093/cercor/bhn181.
Ge, S., Liu, H., Lin, P., Gao, J., Xiao, C., Li, Z., 2018. Neural basis of action observation and understanding from first- and third-person perspectives: an fMRI study. Front. Behav. Neurosci. 12. https://doi.org/10.3389/fnbeh.2018.00283.
Glasser, M.F., Coalson, T.S., Robinson, E.C., Hacker, C.D., Harwell, J., Yacoub, E., Ugurbil, K., Andersson, J., Beckmann, C.F., Jenkinson, M., Smith, S.M., Van Essen, D. C., 2016. A multi-modal parcellation of human cerebral cortex. Nature 536, 171–178. https://doi.org/10.1038/nature18933.
Gothard, K.M., Mosher, C.P., Zimmerman, P.E., Putnam, P.T., Morrow, J.K., Fuglevand, A.J., 2018. New perspectives on the neurophysiology of primate amygdala emerging from the study of naturalistic social behaviors. WIREs Cogn. Sci. 9. https://doi.org/10.1002/wcs.1449.
Hardwick, R.M., Caspers, S., Eickhoff, S.B., Swinnen, S.P., 2018. Neural correlates of action: comparing meta-analyses of imagery, observation, and execution. Neurosci. Biobehav. Rev. 94, 31–44. https://doi.org/10.1016/j.neubiorev.2018.08.003.
Jerjian, S.J., Sahani, M., Kraskov, A., 2020. Movement initiation and grasp representation in premotor and primary motor cortex mirror neurons. Elife 9. https://doi.org/10.7554/eLife.54139.
Jiang, X., Saggar, H., Ryu, S.I., Shenoy, K.V., Kao, J.C., 2020. Structure in neural activity during observed and executed movements is shared at the neural population level, not in single neurons. Cell Rep. 32, 108006. https://doi.org/10.1016/j.celrep.2020.108006.
Keysers, C., Wicker, B., Gazzola, V., Anton, J.-L., Fogassi, L., Gallese, V., 2004. A touching sight. Neuron 42, 335–346. https://doi.org/10.1016/S0896-6273(04)00156-4.
Keysers, C., Kaas, J.H., Gazzola, V., 2010. Somatosensation in social perception. Nat. Rev. Neurosci. https://doi.org/10.1038/nrn2833.
Muthukumaraswamy, S.D., Johnson, B.W., McNair, N.A., 2004. Mu rhythm modulation during observation of an object-directed grasp. Cogn. Brain Res. 19, 195–201. https://doi.org/10.1016/j.cogbrainres.2003.12.001.
Maeda, F., Kleiner-Fisman, G., Pascual-Leone, A., 2002. Motor facilitation while observing hand actions: specificity of the effect and role of observer's orientation. J. Neurophysiol. 87, 1329–1335. https://doi.org/10.1152/jn.00773.2000.
Maranesi, M., Livi, A., Bonini, L., 2015. Processing of own hand visual feedback during object grasping in ventral premotor mirror neurons. J. Neurosci. 35, 11824–11829. https://doi.org/10.1523/JNEUROSCI.0301-15.2015.
Mazurek, K.A., Rouse, A.G., Schieber, M.H., 2018. Mirror neuron populations represent sequences of behavioral epochs during both execution and observation. J. Neurosci. 38, 4441–4455. https://doi.org/10.1523/JNEUROSCI.3481-17.2018.
Mercier, M.R., Dubarry, A.-S., Tadel, F., Avanzini, P., Axmacher, N., Cellier, D., Vecchio, M.D., Hamilton, L.S., Hermes, D., Kahana, M.J., Knight, R.T., Llorens, A., Megevand, P., Melloni, L., Miller, K.J., Piai, V., Puce, A., Ramsey, N.F., Schwiedrzik, C.M., Smith, S.E., Stolk, A., Swann, N.C., Vansteensel, M.J., Voytek, B., Wang, L., Lachaux, J.-P., Oostenveld, R., 2022. Advances in human intracranial electroencephalography research, guidelines and good practices. Neuroimage 260, 119438. https://doi.org/10.1016/j.neuroimage.2022.119438.
Molenberghs, P., Cunnington, R., Mattingley, J.B., 2012. Brain regions with mirror properties: a meta-analysis of 125 human fMRI studies. Neurosci. Biobehav. Rev. 36, 341–349. https://doi.org/10.1016/j.neubiorev.2011.07.004.
Mukamel, R., Ekstrom, A.D., Kaplan, J., Iacoboni, M., Fried, I., 2010. Single-neuron responses in humans during execution and observation of actions. Curr. Biol. 20 (8), 750–756. https://doi.org/10.1016/j.cub.2010.02.045.
Naish, K.R., Houston-Price, C., Bremner, A.J., Holmes, N.P., 2014. Effects of action observation on corticospinal excitability: muscle specificity, direction, and timing of the mirror response. Neuropsychologia 64, 331–348. https://doi.org/10.1016/j.neuropsychologia.2014.09.034.
Ogawa, K., Inui, T., Sugio, T., 2006. Separating brain regions involved in internally guided and visual feedback control of moving effectors: an event-related fMRI study. Neuroimage 32, 1760–1770. https://doi.org/10.1016/j.neuroimage.2006.05.012.
Patuzzo, S., Fiaschi, A., Manganotti, P., 2003. Modulation of motor cortex excitability in the left hemisphere during action observation: a single- and paired-pulse transcranial magnetic stimulation study of self- and non-self-action observation. Neuropsychologia 41, 1272–1278. https://doi.org/10.1016/S0028-3932(02)00293-2.
Perry, A., Stiso, J., Chang, E.F., Lin, J.J., Parvizi, J., Knight, R.T., 2018. Mirroring in the Human brain: deciphering the spatial-temporal patterns of the Human mirror neuron system. Cereb. Cortex. 28, 1039–1048. https://doi.org/10.1093/cercor/bhx013.
Pomper, J.K., Shams, M., Wen, S., Bunjes, F., Thier, P., 2023. Non-shared coding of observed and executed actions prevails in macaque ventral premotor mirror neurons. Elife 12, e77513. https://doi.org/10.7554/eLife.77513.
Qin, C., Michon, F., Onuki, Y., Ishishita, Y., Otani, K., Kawai, K., Fries, P., Gazzola, V., Keysers, C., 2023. Predictability alters information flow during action observation in human electrocorticographic activity. Cell Rep. 42, 113432. https://doi.org/10.1016/j.celrep.2023.113432.
Rizzolatti, G., Fadiga, L., Gallese, V., Fogassi, L., 1996. Premotor cortex and the recognition of motor actions. Cogn. Brain Res. 3, 131–141. https://doi.org/10.1016/0926-6410(95)00038-0.
Rizzolatti, G., Matelli, M., 2003. Two different streams form the dorsal visual system: anatomy and functions. Exp. Brain Res. 153, 146–157. https://doi.org/10.1007/s00221-003-1588-0.
Rizzolatti, G., Cattaneo, L., Fabbri-Destro, M., Rozzi, S., 2014. Cortical mechanisms underlying the organization of goal-directed Actions and mirror neuron-based action understanding. Physiol. Rev. 94, 655–706. https://doi.org/10.1152/physrev.00009.2013.
Rizzolatti, G., Fabbri-Destro, M., Caruana, F., Avanzini, P., 2018. System neuroscience: past, present, and future. CNS. Neurosci. Ther. 24, 685–693. https://doi.org/10.1111/cns.12997.
Shamay-Tsoory, S.G., Mendelsohn, A., 2019. Real-life neuroscience: an ecological approach to brain and behavior research. Perspect. Psychol. Sci. 14, 841–859. https://doi.org/10.1177/1745691619856350.
Turella, L., Tubaldi, F., Erb, M., Grodd, W., Castiello, U., 2012. Object presence modulates activity within the somatosensory component of the action observation network. Cereb. Cortex. 22, 668–679. https://doi.org/10.1093/cercor/bhr140.
Van Essen, D.C., 2012. Cortical cartography and Caret software. Neuroimage 62, 757–764. https://doi.org/10.1016/j.neuroimage.2011.10.077.